96

N91-19209

A Comparative Study of Performance Parameters of n^+-p InP Solar Cells Made by Closed-Ampoule Sulfur Diffusion into Cd- and Zn-Doped p-type InP Substrates

Mircea Faur, Maria Faur, Chandra Goradia and Manju Goradia
*Space Photovoltaic Research Center**
Electrical Engineering Department
Cleveland State University,
Cleveland, OH

Ralph D. Thomas, David J. Brinker, Navid Fatemi** and Frank Honecy
NASA Lewis Research Center
Cleveland OH

Introduction

In previous works [refs. 1,2], we reported a detailed analysis of the InP surface and diffused emitter region of n^+-p InP structures made by thermal diffusion of sulfur into Cd-doped InP substrates. A best 1AM0, 25° efficiency of 14.35% on unoptimized solar cells was obtained. Here we report a comparative study of performance parameters of identically fabricated n+-p InP solar cells made on Cd- and Zn-doped InP substrates with comparable doping and etch pit density. The basic mechanisms which limit the performances of solar cells fabricated on Zn- as compared to Cd-doped substrates are investigated based on structural, compositional and carrier concentration changes in the complex systems In-P-S-O-Zn(Cd) as a result of S diffusion into p-type substrates. Understanding the effects of heat treatment and S diffusion conditions on the above mentioned changes in In-P-S-O-Zn(Cd) systems are essential both in terms of choosing the right substrate, and for optimizing the fabrication steps of n^+-p InP solar cells. The behavior of different species as a result of different processing steps are the key factor to be considered for a better understanding of such complex systems and for a better control of device properties and fabrication. Different diffusing species, e.g. Zn, Cd, S, P, In, on which we report here, have been reported to behave differently in InP and little concensus concerning their diffusion mechanisms and variation with diffusion conditions can be found.

Unlike the relatively large number of papers reporting on acceptor diffusion behavior - especially Zn [refs. 3-6] and, more recently, Cd [refs. 7-9] in InP, very limited information exists on donor behavior, i.e., S diffusion in relation to the other components of In-P-O-S-Cd(Zn) systems. A preliminary investigation of the behavior of such systems under various heat treatment and diffusion conditions, have enabled us 1) to explain the differences in performances of solar cells made on Zn-and Cd-doped

*Funded by NASA Lewis Research Center
**Sverdrup Technology, Inc., Lewis Research Center Group

substrates, and 2) to gather new data on Cd, Zn and S diffusion mechanisms in InP for optimizing the closed ampoule diffusion of sulfur into p-type InP. Part of the results of this study are reported here.

Experimental

A closed-ampoule technique was used to fabricate n^+-p structures by thermal diffusion of sulphur into p-type InP substrates. The surface preparation prior to diffusion, closed-ampoule diffusion environment and conditions, and post-diffusion preparation procedures have been previously reported [ref. 1]. The substrates used were Czochralski (LEC) grown Cd-and Zn-doped from Crystacomm, Inc. and Nippon Mining Co. The doping, etch pit density, and other characteristics of these materials have been measured prior to and/or after heat treatment or diffusion by using Van der Pauw Hall effect and Scaning Electron Microscopy (SEM) data analysis. Atomic and carrier concentration depth profiles have been obtained by Auger Electron Spectroscopy (AES) and electrochemical C-V (ECV) measurements using a Polaron profiler (type PN 420Q). The changes in chemical composition of heat treated or diffused surfaces have been extracted from X-ray Photoelectron Spectroscopy (XPS) data.

Small area n^+-p InP unoptimized solar cells were fabricated under identical conditions, on structures made by thermal diffusion of S into Cd- and Zn-doped substrates. Electron beam evaporated Au-Zn-Au back contacts were sintered in forming gas for 3 minutes at 425°. The front contacts were 2000Å thick Au, evaporated by using photolithographically defined pattern. The grid shadowing was 6.25%. About 800Å thick SiO was used as an anti-reflection (AR) coating. Small area (0.48 cm^2) solar cells were defined by mesa etching.

Results and Discussion

A comparative study of performance parameters of identically fabricated n^+-p InP solar cells made by closed ampoule S diffusion into p-type InP is presented in Table 1. The total area AM0, 25° solar cell performance parameters were measured at NASA LeRC. As seen, the best efficiency is 11.83% for Zn-doped substrates as compared to 14.35% for Cd-doped substrates. For the three diffusion temperatures no significant differences exist between the values of V_{oc} and J_0. However, I_{sc}, FF and R_s vary more substantially for the two substrates. An explanation of these differences is given next in terms of structural, chemical and electrical changes we have observed in In-P-S-O-Zn(Cd) systems after thermal treatment and diffusion.

Heat Treatment Effects

In order to undetand the structural and electrical changes in p-type InP after diffusion, we have heat treated clean Cd-and Zn-doped substrates in evacuated closed

ampoule. As seen in Figure 1, after 3 hours of heat treatment at 660°, the decrease in either P or In surface concentration is relatively small and it is believed to be mainly due to C and O impurities detected at the surface. It is known that InP surface decomposes incongruently at temperatures greater than 356°C [ref.10]. Because a large number of P vacancies (V_P) are created at the surface as an effect, various neutral complexes such as X_{In} V_P or $V_P X_{In} V_P$ are formed [refs. 3,4], where X_{In} represent either Zn_{In} or Cd_{In}. In the $V_P X_{In} V_P$ complex mechanism, one In vacancy, V_{In}, and two P vacancies, V_P, are used up every time an interstitial Zn or Cd atom forms a complex. Since the Zn-doped substrate shows a more severely P depleted region as compared to the Cd-doped one, we assume that a much larger number of neutral complexes are formed in the Zn-doped substrate as compared to the Cd-doped substrate. This is confirmed by the In accumulation at the thin front oxide layer - InP:Zn interface, as seen in Figure 1b.

As previously reported for the InP:Zn substrates [refs. 11-14], an increase in hole density was observed for both Cd-and Zn-doped heat treated substrates, as shown in Figure 2. For Zn-doped substrates the effect was explained in terms of outdiffusion of interstitial Zn donors, thus decreasing the compensation of substitutional Zn acceptors [ref. 13]. This could be the case since the ECV profiles do not seem to follow the variation of In Auger profiles. Hence, the small increase in concentration of substitutional Zn_{In-} acceptors is not expected to account for the relatively large increase in measured acceptor concentration.

In the case of highly doped InP:Zn (1.2 E18 cm^{-3}), however, a very large increase in acceptor concentration appears toward the surface after 3 hours of heat treatment at 660°C as seen in Figure 3. The higher acceptor concentration near the surface with increased background doping can be explained by the increasing substitutional Zn_{In-} concentration added to a constant Zn complex solubility. This could be interpreted as being due to the interaction of singly ionized Zn interstitial not with neutral In vacancies, V_{In}, but with negatively charged In vacancies, V_{In-}, which could be more numerous than neutral vacancies in highly doped p-type InP.

From the above experiments, and assuming a constant Zn solubility which is to be expected for constant new created In and P vacancy concentrations, under similar heat treatment conditions, we concluded that 1) a large accumulation of neutral complexes are expected to appear at the surfaces in the case of low doped materials, while 2) the large accumulation of Zn at the surface in highly doped substrates is mainly due to Zn_{In-} acceptor formation.

Hall effect measurements of bulk acceptor concentration prior to and, after heat treatment at 660°C for 3 hours in the case of low doped Zn-and Cd-doped InP substrates, and 2 hours for the highly Zn-doped substrate, presented in Table 2, show a good agreement with C-V data presented in Figs. 2 and 3. The discrepancy in the case of highly doped substrates is due to differences in heat treatment time, i.e. 3 hours for the case of ECV data and 2 hours in the case of Hall effect data. Also shown

in Table 2 are values of resistivity (ρ) and mobility (μ). As expected with increasing hole concentration both ρ and μ decrease.

From the ECV and Hall effect data it is apparent that the increase in acceptor concentration, as a result of heat treatment is smaller in the case of InP:Cd as compared to InP:Zn of similar doping. This suggests that the interstitial Cd is present in much smaller densities as compared to interstitial Zn since as we have shown before, the density of neutral species also appear to be much smaller in the case of Cd doped materials.

Dislocation Density

The high dislocation density of S diffused InP surfaces are due to: 1) propagation of dislocations initially present in the substrates, 2) formation and propagation of dislocations from precipitates initially present in the crystal and 3) precipitates introduced during diffusion. Taking into consideration that dislocation motion will never occur without breaking crystal bonds, it is reasonable to assume that the bond strength plays an important role in the dislocation motion [ref. 15]. Judging from their high diffusivity, interstitial Zn atoms are not presumed to form strong bonds with host crystal atoms which surround the Zn atoms. Thus, the interstitial Zn atoms will not behave as a pinning point for dislocation motion. If the strength of bonds being formed between doped impurity atoms and sublattice site atoms, which surround the doped impurity atoms, is large enough, propagating dislocations are expected to be pinned at the impurity position. Thus, propagating dislocations under a driving force, i.e. thermal stress introduced during thermal diffusion will be stopped at a position adjacent to the impurities, provided the impurity forms strong bonds with one of the constituent atoms of the host crystal.

We have previously reported [ref. 2] that In_xS_y droplets appear on the surface of InP after closed-ampoule S diffusion into Cd-doped substrates at all diffusion temperatures from 600 to 725°C. These droplets, as seen in Figure 4, accumulate at the defect areas, i.e. at the etch pits at diffusion temperature of up to 700°C (see fig. 4a), and along the microcracks at higher temperatures as can be seen in Figs. 4c and 4d. The droplet density is indicative of dislocation density increase as the diffusion temperature or times increase from 600 to 700°C and from 1 to 4 hours, respectively.

For Zn-doped materials, under similar diffusion conditions, the droplet density has been found to be much higher than in the case of Cd-doped substrates. As seen in Table 3, the increase in dislocation density for Zn-doped substrates, after 3 hours diffusion at 660°C is more than one order of magnitude higher as compared to Cd-doped substrates. The differences observed in the values of EPD_d/EPD_0 ratios for NMC and CCI Zn-doped crystals can be due to inaccuracies in counting the droplets or to a larger number of precipitates initially present in the NMC crystal, probably due to the higher doping concentration.

Prior to diffusion, Cd-and Zn-doped substrates used in this study had comparable etch pit densities (EPD), as seen in Figure 5. The EPDs on virgin surfaces were slightly higher than 2E5/cm^2. However, after surface preparation prior to diffusion, including the removal of about 10μm damaged layer in Br_2-methanol (0.5% Br_2) solution, the EPDs for Zn doped materials were about 5 and 7×10^4/cm^2 and of about 7×10^4/cm^2 for Cd-doped substrates, respectively, as shown in Table 3.

Following a similar post-diffusion surface preparation procedure as reported for the case of Cd-doped substrates [ref. 2] the droplets accumulation from the Zn-doped surfaces could not be removed, as seen in Fig. 6a. For comparison, in the case of Cd-doped substrates, the micrograph in Fig. 4b shows the same location of surface as in Fig. 4a after post-diffusion surface preparation.

SEM analysis of surface topography in the case of Zn-doped substrates, after thinning down the n^+ emitter layer by anodic dissolution,have shown that the In_xS_y precipitate density decreases from about 2×10^7 /cm^2 at the surface to zero at the junction depth. Figure 6c represents a view of surface topography after removal of about 1,200Å thick layer from the surface of Fig. 6a. In contrast, a S diffused Cd-doped substrate, with a 600Å front surface removed, shows no sign of In_xS_y precipitates. The micrograph in Fig. 6b shows the surface dislocatlon density of structure in Fig. 6a, as revealed electrochemically in O-H_3PO_4 (0.5M) solution.

From these experiments it is apparent that the In_xS_y-rich precipitates are present only at the surface in the case of Cd-doped substrates and decrease exponentially from the surface value to zero in the vicinity of the junction in the case of Zn-doped substrates.

The exact composition of In_xS_y precipitates could not be identified, but EDAX and XPS analysis have shown that they are rich in In and S [ref. 2]. From the phase diagram [ref. 16] three stable compounds could be formed in In-S system under the diffusion conditions, e.g. In_2S_3, InS and In_6S_7. However, in the case of Zn-doped substrates, Zn precipltates could appear as a result of heat treatment [refs. 17-18]. We assume that these precipitates contrary, to In precipitates which are believed to concentrate at the surface, can be distributed inside the bulk material. This assumption can provide an explanation for the differences observed in the density and distribution of these precipitates in the case of Zn-and Cd-doped substrates.

AES and ECV Depth Profiles

In Figure 7 are presented S, P and In AES depth profiles after 3 hours closed-ampoule S diffusion into Cd-doped InP substrates at different diffusion temperatures [ref. 2]. As expected the S profiles are temperature dependent and it is clear that the severely P-depleted front surface region is mainly due to the substitution of P by S in the host InP lattice, rather than due to $V_PCd_{In}V_P$ neutral complex formation. For diffusion temperatures of 650 to 700°C, the S concentration is nearly constant

up to depths of several hundred angstroms. The anomalous behavior at 675°C has been explained by the formation at this temperature, of a stable glass-like $In(PO_3)_3$ polyphosphate at the surface, as revealed by XPS data [ref. 2], which acts as a diffusion barrier. The increased concentration of In at the oxide/n^+ interface is assumed to be due, as stated before, to In_xS_y-rich precipitate formation. The S profiles also show an increase in concentration at this location.

In the case of S diffusion into Zn-doped substrates, as seen in Figure 8, P profiles show a more severe loss of phosphorus and, as a consequence, a deeper junction depth, as compared to diffusions into Cd-doped substrates. A deeper junction depth, however, is expected since an increase in diffusion-induced dislocations, which act as P vacancy generators, could form diffusion pipes. However, by increasing the amount of added phosphorus to the ampoule, the phosphorus loss is diminished and, as a consequence, the S profiles vary accordingly. The accumulation of In at the oxide/n^+ interface is associated to the formation of $Zn_{In}-$, and the In depletion to outdiffusion of interstitial In. The deep accumulation of In is presumed to be due to the diffusion of interstitial In, and In precipitates accumulation at the dislocation areas, due especially to the formation of neutral complexes $V_PCd_{In}V_P$.

The ECV thermal equilibrium majority carrier concentration depth profiles after S diffusion into Cd-doped substrates, have essentially similar shapes as S atomic concentration Auger profiles. However, in the case of Zn-doped substates, the C-V and Auger profiles are quite different. Figure 9 shows two C-V depth profiles after 3 hours S diffusion into the two substrates. As seen, a nearly step diffusion profile is obtained in the case of diffusion into Cd-doped substrate, while a graded profile is seen in the case of diffusion into Zn-doped substrate. The discrepancy is explained based on the differences between the dislocation densities introduced during S diffusion into the two substrates. In the case of diffusion into Cd-doped substrates it seems that most of the S is found in ionized form and appears as a donor. In the case of Zn-doped substrates, however, the departure of C-V profile from a nearly step Auger profile can be explained by assuming that a part of sulfur combines with interstitial In and, probably, Zn and forms stable In_xS_y or ZnS precipitates at the dislocation regions.

External Quantum Efficiency

The last characteristic we discuss here in an attempt to explain the differences between the performance parameters of solar cells fabricated on Zn- and Cd-doped substrates is the external quantum efficiency (EQE).

Figure 10 presents the variation of EQE for solar cells fabricated by 3 hours S diffusion into Cd- and Zn-doped substrates at two diffusion temperatures of 625°C and 660°C.

At the diffusion temperature of 625°C no significant differences could be seen from the EQE variations which could explain the differences in performance parameters shown in Table 1. Then the differences in performance parameters, especially I_{sc} and FF, could be related to an increase observed in the series resistance (R_s) in the case of Zn-doped substrates.

In the case of diffusions at 660°C, however, the EQE variations for the two substrates are in good agreement with differences between the ECV and AES depth profiles and which are explained in terms of a higher dislocation density in the case of Zn-doped substrates. The electrically inactive S, which is incorporated into In_xS_y, and probably, ZnS precipitates at the dislocation regions, will produce a dead layer near the surface. As shown in the previous sections, in the case of Cd-doped substrates, the dead layer is superficial and can be removed by an appropriate post-diffusion surface preparation. In the case of Zn-doped substrates, the dead layer extends well below the surface. This explains the decrease in I_{sc} and increase in R_s since the presence of a dead layer will reduce the collection efficiency by reducing the minority-carrier lifetimes. The decrease in FF is related to the increase in R_s value, which is mainly due to an increased sheet resistivity.

Conclusion

Our preliminary results indicate that Cd-doped substrates are better candidates for achieving high efficiency solar cells fabricated by closed-ampoule S diffusion than Zn-doped substrates. The differences in performance parameters (i.e. 14.35% efficiency for Cd-doped vs. 11.83% in the case of Zn-doped substrates of comparable doping and EPDs) have been explained in terms of a large increase in dislocation density as a result of S diffusion in the case of Zn-doped as compared to Cd-doped substrates. The In_xS_y and probably, ZnS precipitates in the case of Zn-doped substrates, produce a dead layer which extends deep below the surface and strongly affect the performance parameters.

It should be noted that our cells had an unoptimized single layer AR coating of SiO, a grid shadowing of 6.25% and somewhat poor contacts, all contributing to a reduction in efficiency. We believe that by reducing the external losses and further improvement in cell design, efficiencies approaching 17% at 1AM0, 25° should be possible for cells fabricated on these relatively high defect density Cd-doped substrates. Even higher efficiencies, 18-19% should be possible by using long-lifetime substrates and further improving front surface passivation. If solar cells fabricated on Cd-doped substrates turn out to have comparable radiation tolerance as those reported in the case of cells fabricated on Zn-doped substrates, then for certain space missions 18% to 19% efficient cells made by this method of fabrication would be viable.

References

[1.] Mircea Faur, Maria Faur, Chandra Goradia, Manju Goradia, Navid Fatemi, David Brinker and Ralph Thomas, *1st Int. Conf. on InP and Related Materials*, 1989.

[2.] Maria Faur, Mircea Faur, Manju Goradia, Chandra Goradia, Douglas Jayne, Frank Honecy and Irving Weinberg, *1st Int. Conf. on InP and Related Materials*, 1989.

[3.] B. Tuck and A. Hooper, J. Phys. **D8**, 1806, 1975.

[4.] A Hooper and B. Tuck, Solid State Electron. **19**, 513, 1976.

[5.] H. B. Serreze and H. S. Marek, Appl. Phys. Lett. **49**, 210, 1986.

[6.] G. J. van Gurp, P. R. Boudewijn, M. N. C. Kempeners and D. L. A. Tjaden, J. Appl. Phys. **61**, 1846, 1987.

[7.] P.K. Tien and B.I. Miller, Appl. Phys. Lett. 34 **10**, 701, 1979.

[8.] H. Ando, N. Susa and H. Kanbe, IEEE Trans. on Elecl ron Devices, **ED-29**, 1408, 1982.

[9.] K. Ohtsuka, T. Matsui and H. Ogata, Jpn. J. Appl. Phys. **27**, 253, 1988.

[10.] R.F.C. Farrow, J. Phys. **D7**, 2436, 1974.

[11.] K. Tsubaki and K. Sugiyama, Jpn. J. Appl. Phys. **19**, 1185, 1980.

[12.] K. Tsubaki and K. Sugiyama, Jpn. J. Appl. Phys. **19**, 1789, 1980.

[13.] C.C.D. Wong and R.H. Bube, J. Appl. Phys. **55**, 3804, 1984.

[14.] H.S. Marek and H.B. Serreze, Appl. Phys. Lett. **51**, 2031, 1987.

[15.] Y. Seki, H. Watanabe and J. Matsui, J. Appl. Phys. **49**, 822, 1978.

[16.] H.G. Ansell and R.S. Boorman, J. Electrochem. Soc. **118**, 133, 1971.

[17.] S. Mahajan, V.A. Bonner, A.K. Shin, and D.C. Miller, Appl. Phys. Lett. **35**, 165, 1979.

[18.] R.S. Williams, P.A. Barnes, and L.C. Feldman, Appl. Phys. Lett. **36**, 760, 1980.

Table I: Comparison of solar cell performance parameters[a] for cells fabricated on Zn- and Cd-doped substrates

Cell[b]	J_{sc}[c] (mA/cm^2)	V_{oc} (mV)	FF (%)	η (%)	$J_0(A=1)$ (A/cm^2)	R_s (Ω-cm^2)
DZ-3-600	27.96	799	65.4	10.66	8.23E-16	5.15
DC-3-600	29.5	803	76.9	13.28	7.82E-16	2.12
DZ-3-625	27.67	811	68.7	11.24	5.78E-16	3.34
DC-3-625	28.94	809	74.1	12.66	6.08E-16	1.44
PDZ-3-660	26.93	813	74.1	11.83	4.93E-16	5.36
PDC-3-660	30.48	806	80.1	14.35	5.50E-16	1.07

[a] All cell measurements were performed at NASA LeRC, under AM0, 25°C conditions.
[b] Notation DZ(C)-3-X stands for Diffusion into Zn(Cd)-doped substrates for 3 hours at diffusion temperature X(°C). An initial P indicates that substrates were Passivated prior to diffusion.
[c] total cell area 0.6cm × 0.8cm = 0.48cm. $I_{sc} = 0.48 J_{sc}$.

Table 2: Resistivity ρ, mobility μ, and doping N_a for Zn- and Cd-doped substrates from Crystacomm Inc.(CCI) and Nippon Mining Co.(NMC) before and after 3 hours heat treatment (2 hours for NMC crystal) at 660°C in closed-evacuated quartz ampoule.

Vendor	Dopant	Before heat treatment			After heat treatment			
		ρ_0, $\times 10^{-2}$ Ω-cm	μ_0, cm^2/V-sec	N_a^0, $\times 10^{16}$ cm^{-3}	ρ_h, $\times 10^{-2}$ Ω-cm	μ_h, cm^2/V-sec	N_a^h, $\times 10^{16}$ cm^{-3}	$\frac{N_a^h}{N_a^0}$
CCI	Zn	425.5	141.9	1.03	95.9	138.5	4.7	4.54
CCI	Cd	479.7	154.9	1.07	158.1	145.0	2.7	2.52
NMC	Zn	6.7	77.7	120.0	3.7	69.0	246.5	2.05

Table 3: Approximate density of etch pits on p-type InP substrates after removing about 10 μm from the surfaces in Br_2-methanol (EPD_0), and after closed-ampoule S diffusion for 3 hours at 660°C (EPD_d).

Vendor	Dopant	N_a, $\times 10^{16}$ cm^{-3}	EPD_0, $\times 10^4$ cm^{-2}	EPD_d, $\times 10^6$ cm^{-2}	$\frac{EPD_d}{EPD_0}$
NMC	Zn	2.24	5	22	440
CCI	Zn	1.03	7	20	330
CCI	Cd	1.07	7	2.3	29

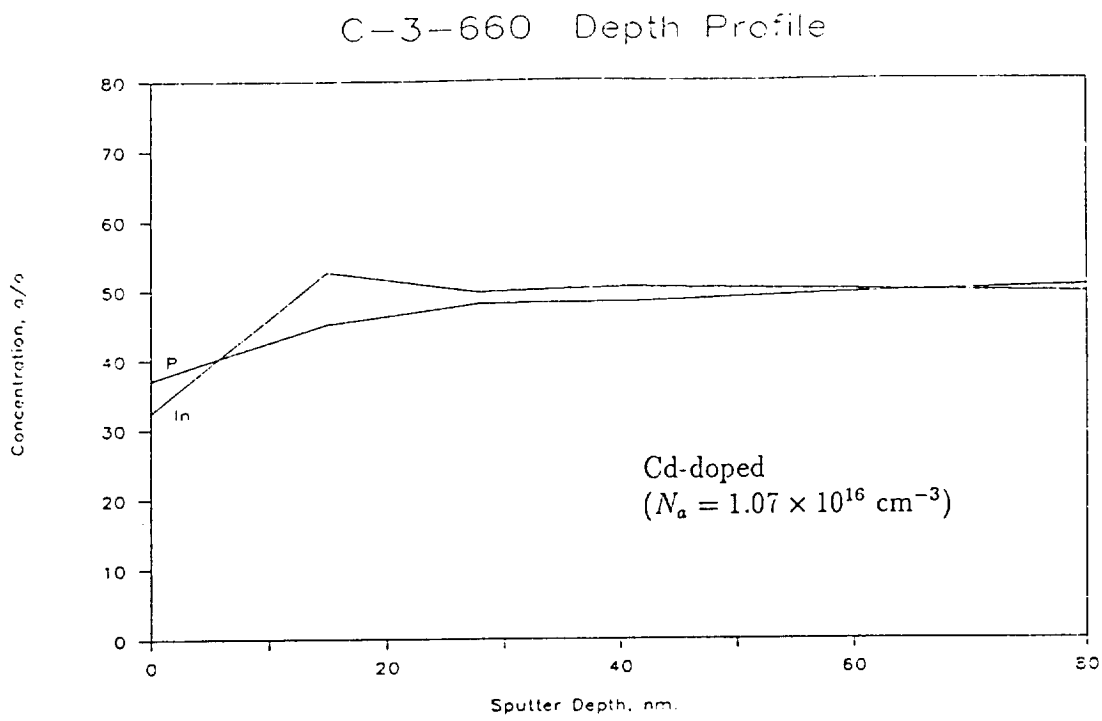

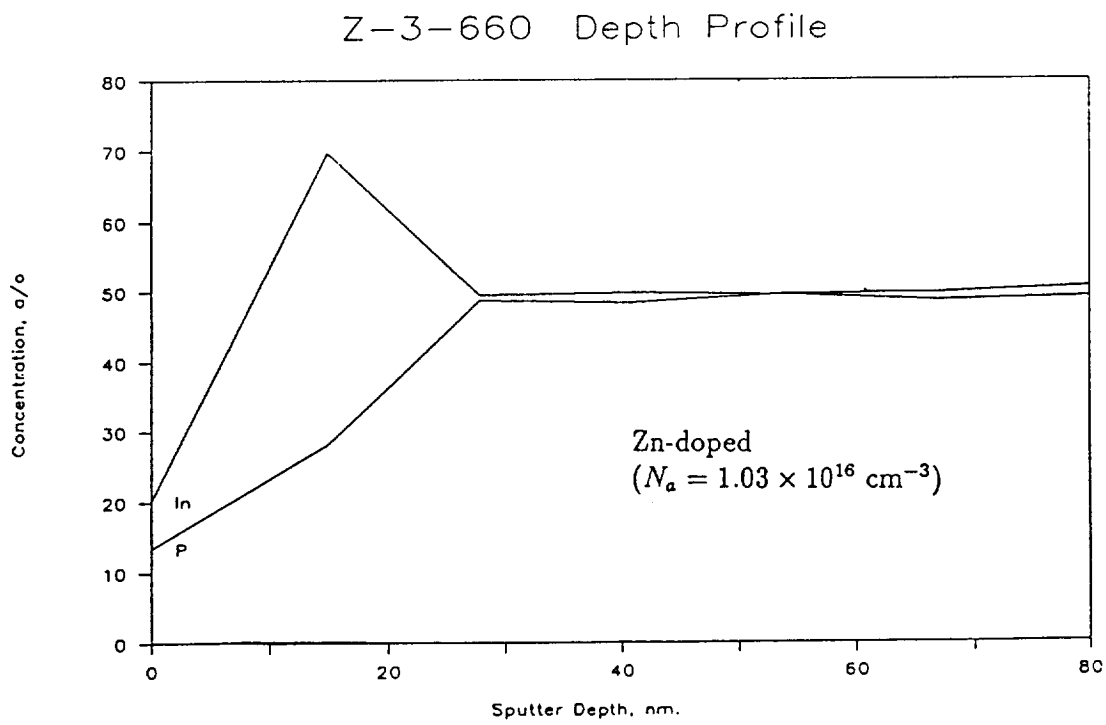

Figure 1. P and In AES profiles after 3 hours closed-ampoule heat treatment of clean Cd- and Zn-doped InP substrates.

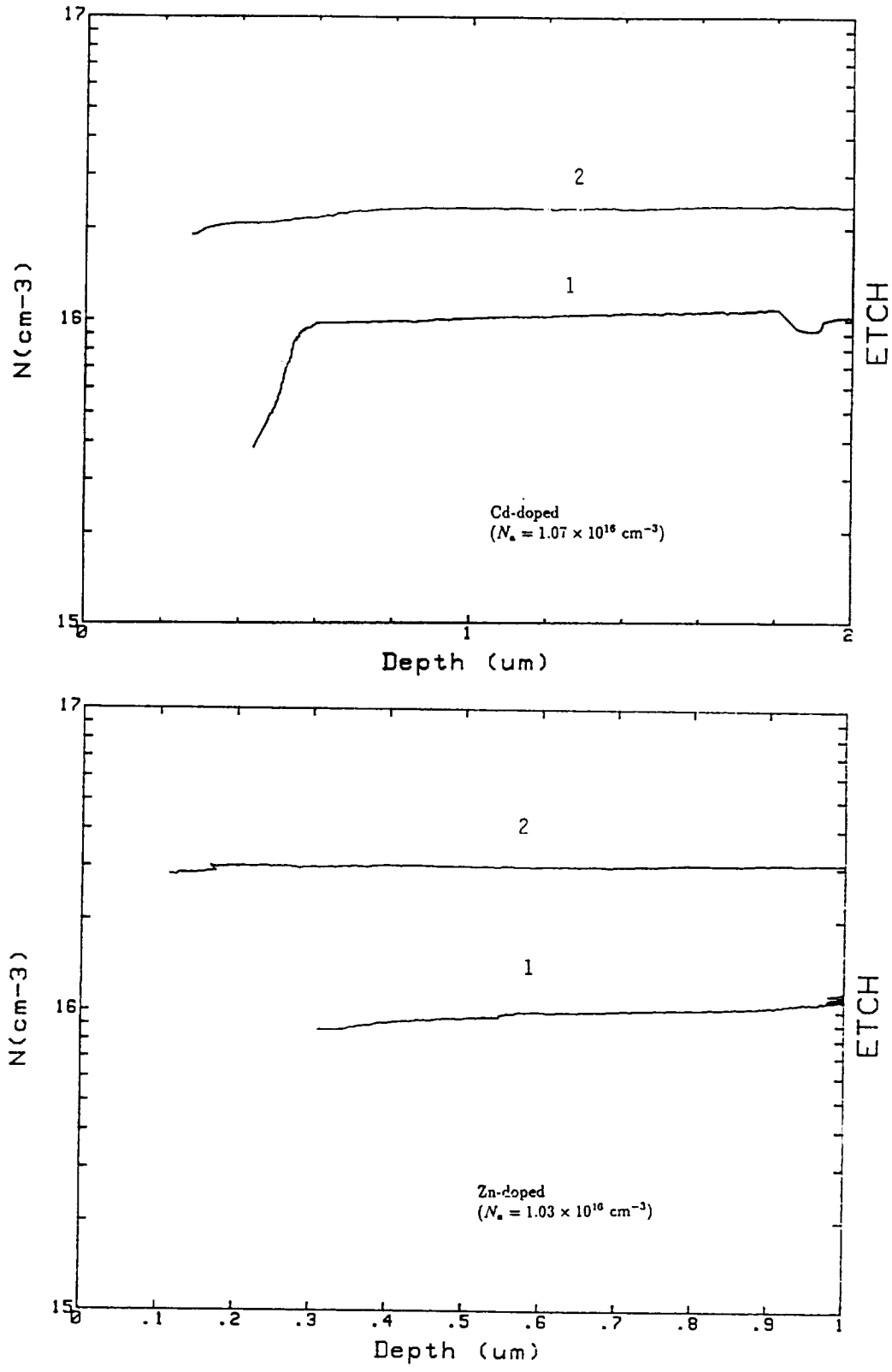

Figure 2. ECV acceptor concentration profiles before (curves 1) and after (curves 2) 3 hours heat treatment at 660°C of clean Cd- and Zn-doped InP substrates.

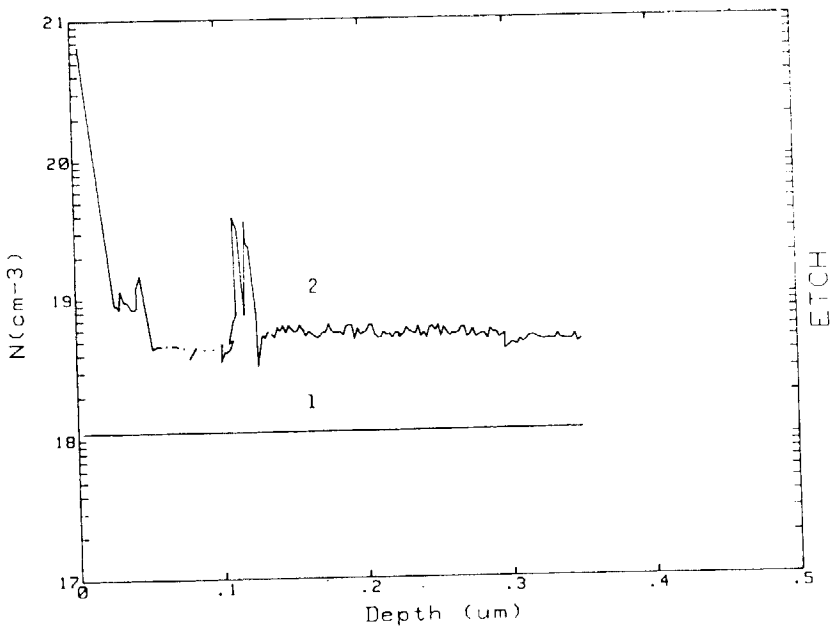

Figure 3. ECV acceptor concentration profiles before (curve 1) and after (curve 2) 3 hours heat treatment at 660°C of Zn-doped ($N_a = 1.2 \times 10^{18}$ cm^{-3}) InP substrates.

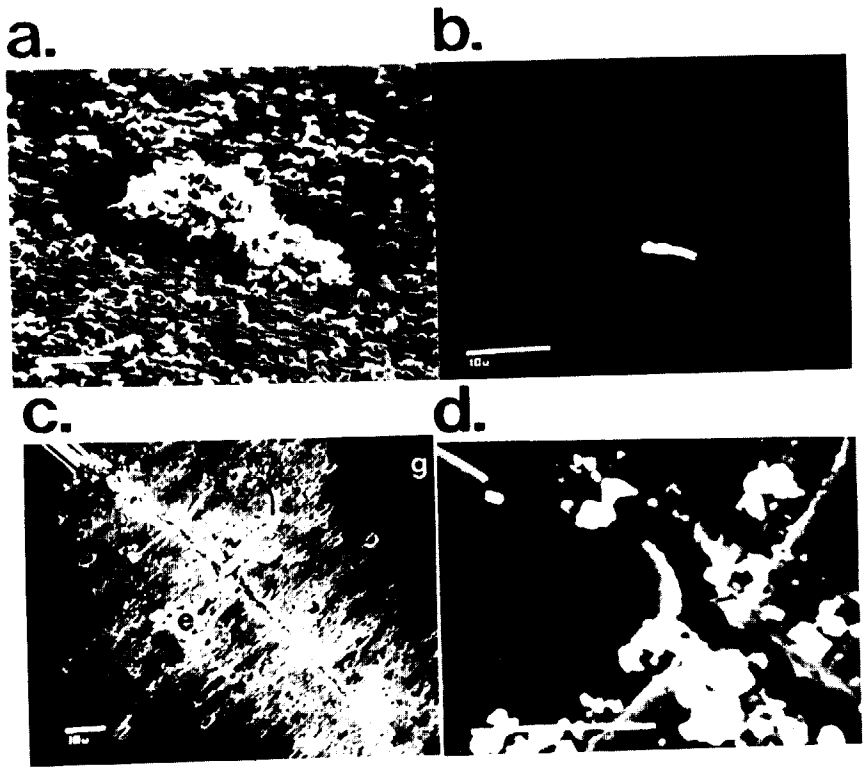

Figure 4. In_xS_y droplet accumulation on surface after 3 hours S diffusion into Cd-doped InP; a) at a temperature of 675°C; b) same region of Fig. 4a after droplet removal; c) at a temperature of 725°C and d) enlarged view of the center region of Fig. 4c.

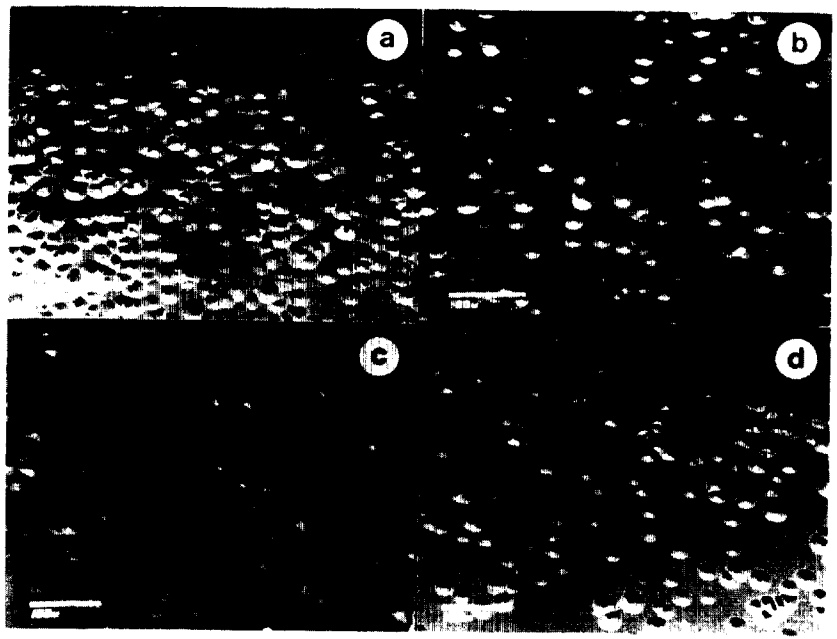

Figure 5. Etch pit density (EPD) revealed after two minutes etching in O-H_3PO_4:HBr (2:1) for a) NMC, Zn-doped (2.24×10^{16} cm^{-3}) InP substrate, b) same substrate after removal of about 10 μm in Br_2-methanol; and CCI, c) Cd-doped (1.07×10^{16} cm^{-3}), and d) Zn-doped (1.03×10^{16} cm^{-3}) after 10 μm removal in Br_2-methanol

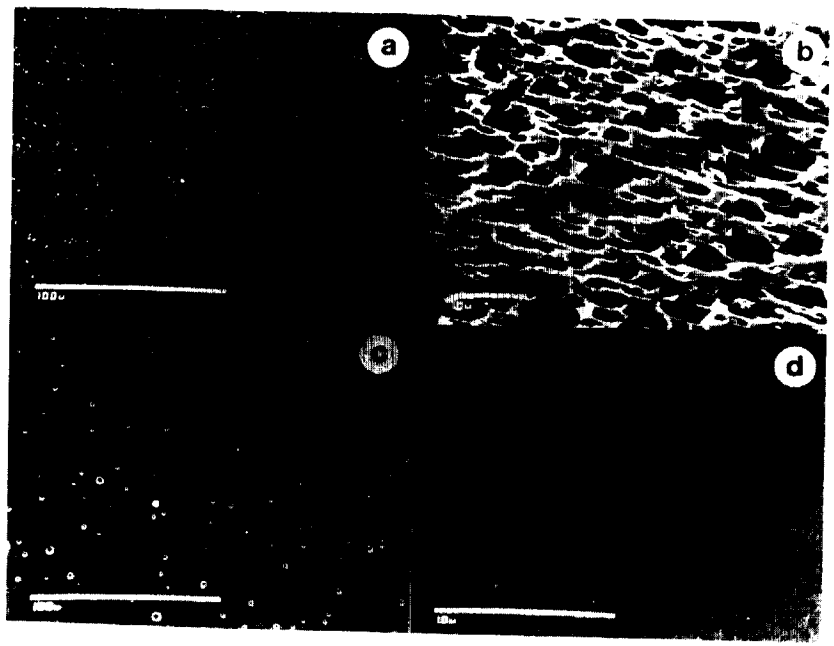

Figure 6. SEM surface topography after 3 hours S diffusion into Zn-doped (1.03×10^{16} cm^{-3}) substrates: a) after same surface treatment as in fig. 4b; b) electrochemically revealed EPD of surface in Fig 6a, in O-H_3PO_4 (0.5M) solution; c) surface in Fig. 6a after anodic disolution to a depth of about 120 nm; d) surface of a n^+p structure S-diffused for 3 hours at 660°C into Cd-doped substrate, after anodic dissolution to a depth of about 60 nm.

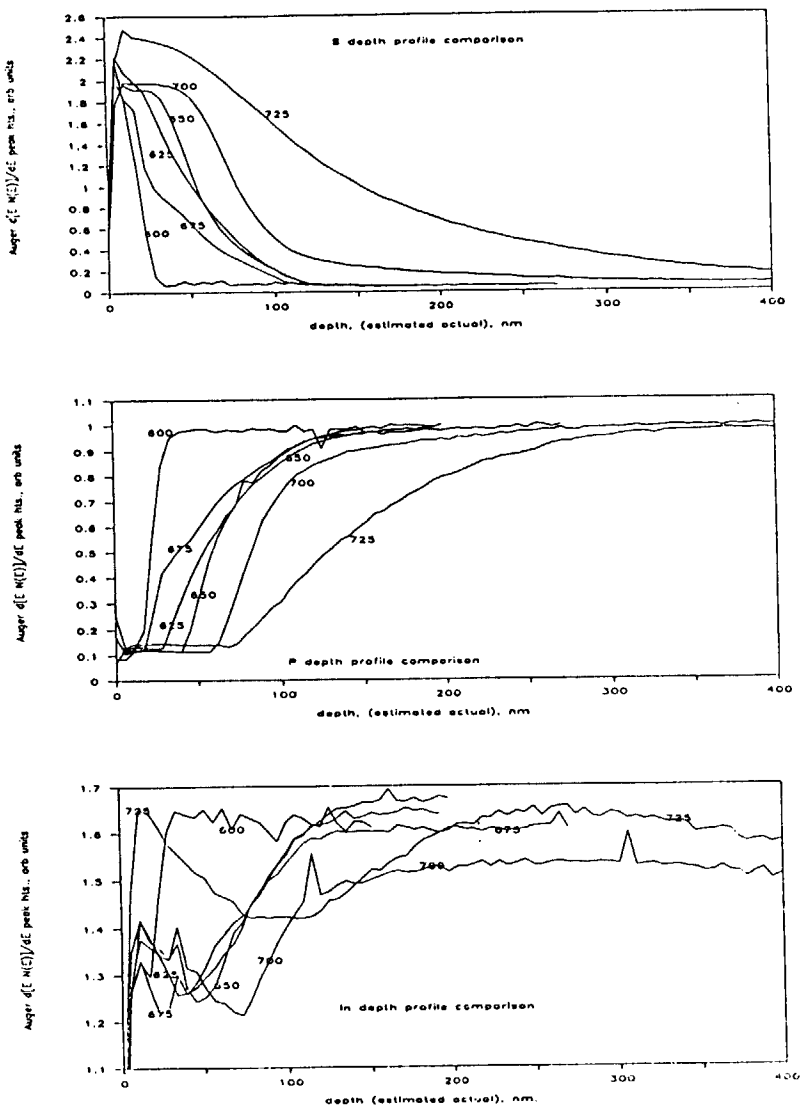

Figure 7. S, P and In AES depth profiles after 3 hours closed-ampoule S diffusion into Cd-doped ($N_a = 1.07 \times 10^{16}$ cm^{-3}) InP substrates, at different diffusion temperatures.

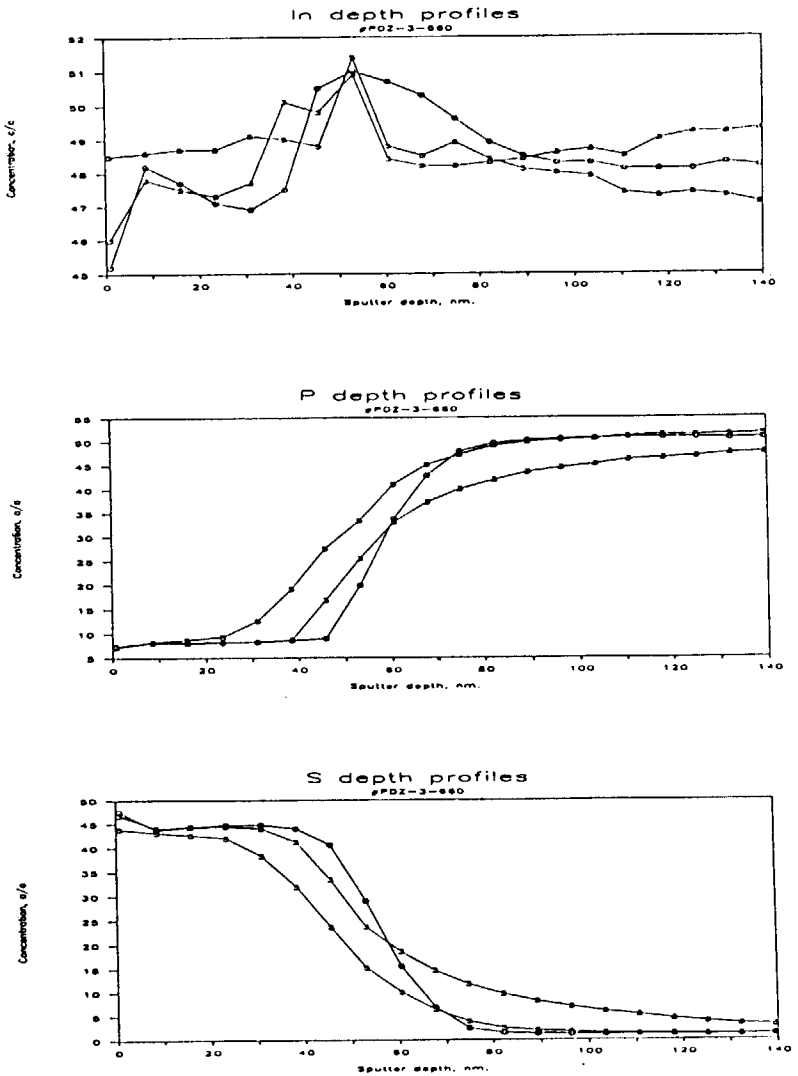

Figure 8. In, P and S AES depth profiles after 3 hours closed-ampoule S diffusion at 660°C. The parameter is the amount of red phosphorus added to the ampoule (in mg).

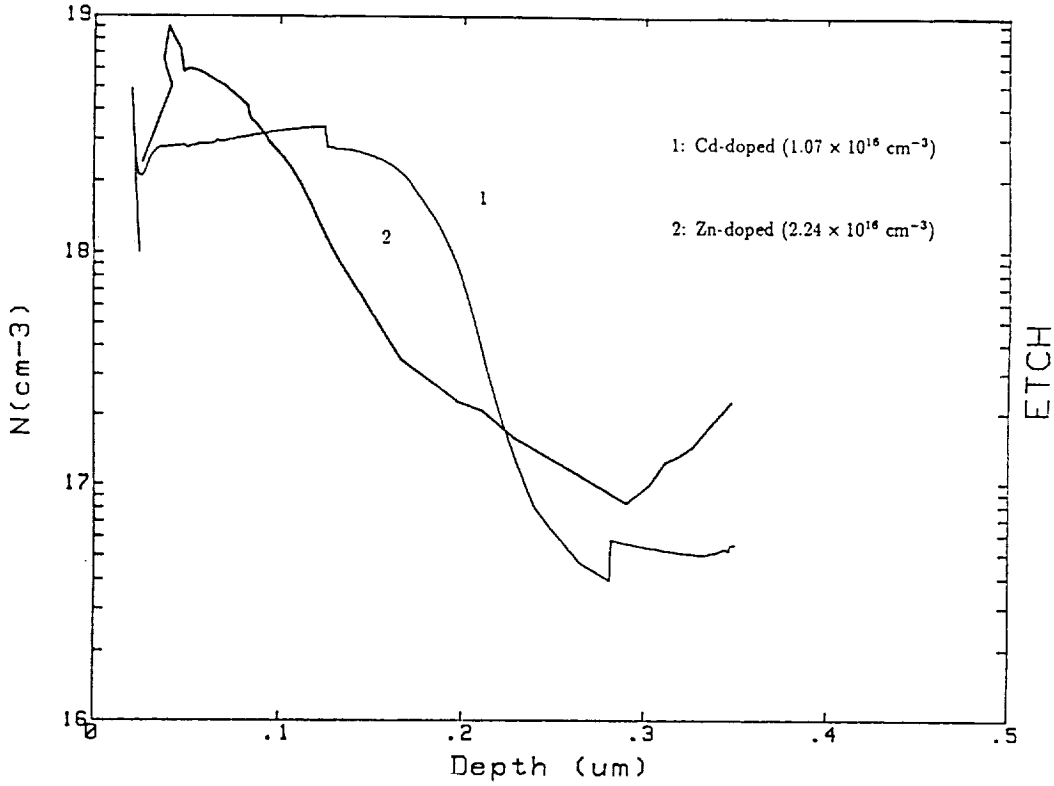

Figure 9. ECV thermal equilibrium majority carrier concentration depth profiles after S diffusion into Cd- and Zn-doped InP substrates, for 3 hours at 660°C.

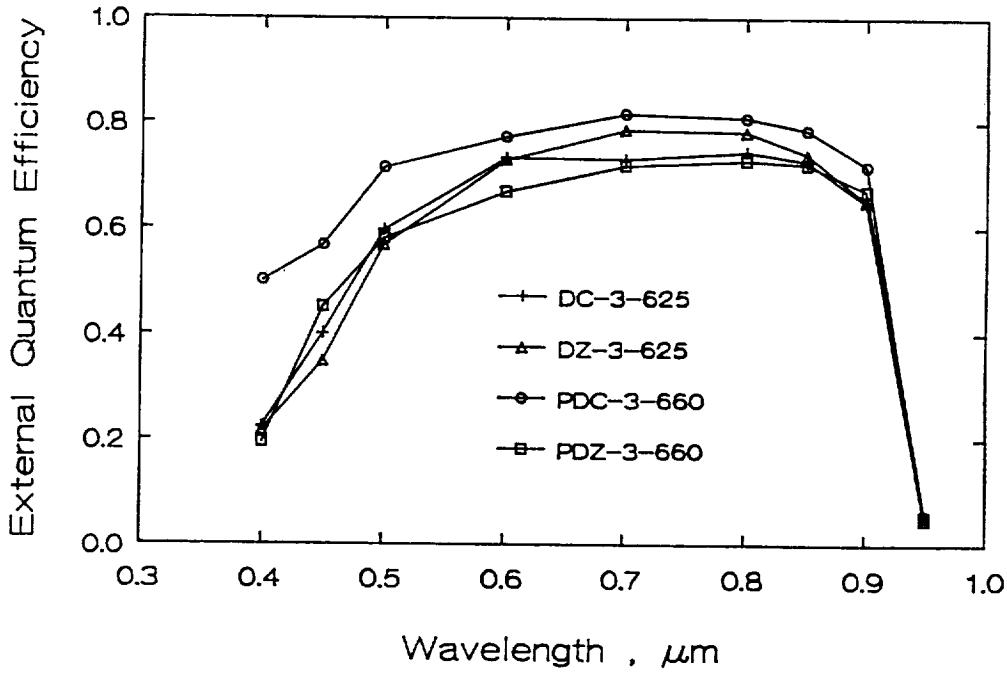

Figure 10. External Quantum Efficiency for solar cells fabricated on Cd- and Zn-doped substrates with performance parameters shown in Table 1.

Session 5
Non-Solar Direct Conversion